

# Cuprous oxide-based nanocrystals with combined chemo/chemodynamic therapy to increase tumor drug sensitivity by reducing mitochondria-derived adenosine-triphosphate

Haoran He<sup>at</sup>, Jiaming Wu<sup>bt</sup>, Min Liang<sup>ct</sup>, Yao Xiao<sup>c</sup>, Xuejian Wei<sup>a</sup>, Yuqin Cao<sup>a</sup>, Zhiheng Chen<sup>bt</sup>, Tian Lin<sup>d</sup> and Miaosheng Ye<sup>a</sup>

<sup>a</sup>The Second People's Hospital of Nanhai District, Guangdong Provincial People's Hospital's Nanhai Hospital, Foshan, Guangdong Province, China; <sup>b</sup>Department of Gastrointestinal Surgery, The First Affiliated Hospital of Jiaying University, Jiaying, Zhejiang Province, China; <sup>c</sup>Department of Oncology, Innovation Centre for Advanced Interdisciplinary Medicine, Guangzhou Key Laboratory of Enhanced Recovery after Abdominal Surgery, The Fifth Affiliated Hospital of Guangzhou Medical University, Guangzhou Medical University, Guangzhou, Guangdong Province, China; <sup>d</sup>Nanfeng Hospital, The First School of Clinical Medicine, Southern Medical University, Guangzhou, Guangdong Province, China

## ABSTRACT

Gastrointestinal (GI) tumor is a serious disease with high mortality rates and morbidity rates worldwide. Chemotherapy is a key treatment for GI, however, systematic side effects and inevitable drug resistance complicate the situation. In the process of therapy, P-glycoprotein (P-gp) could remove chemotherapy drugs from cells, thus causing multi-drug resistance. Chemodynamic therapy (CDT) utilizing Fenton chemistry has been used for cancer therapy, along with various combination therapies. The reactive oxygen species produced by CDT could inhibit P-gp's efflux pump function, which reduce chemoagents excretion and reverse drug resistance. In the present study, we developed novel nanocrystals (Cu<sub>2</sub>O@Pt NCs) to overcome drug resistance by reducing mitochondria-derived ATP through chemo/CDT in GI cancer. Furthermore, *in vivo* results in tumor-bearing mice demonstrated that treatment with Cu<sub>2</sub>O@Pt NCs with CDT and chemotherapy could achieve the most effective antitumor therapeutic effect with the least amounts of adverse effects. As a result, Cu<sub>2</sub>O@Pt NCs could provide a promising strategy for chemo/CDT-synergistic therapy.

## ARTICLE HISTORY

Received 11 July 2022  
Revised 25 August 2022  
Accepted 29 August 2022

## KEYWORDS

Cuprous oxide (Cu<sub>2</sub>O); drug resistance; P-glycoprotein (P-gp); chemodynamic therapy (CDT); mitochondria damage


## 1. Introduction

Gastrointestinal (GI) tumor is one of the five most common cancer types in the world and the major contributor to cancer-related death worldwide (Bray et al., 2018; Sung et al., 2021). To date, surgery remains the mainstay of GI tumors treatment, and it is a trend to shift to minimally invasive surgery (Akahoshi et al., 2018). Meanwhile, given either pre-operatively or postoperatively, adjuvant chemotherapy could improve survival compared with surgery alone because 80% of patients with GI cancer are diagnosed in the advanced stage (Venerito et al., 2016; Chen et al., 2021). Although the optimum chemotherapy regiment is the traditional platinum (Pt)-based chemotherapy, the effectiveness is dramatically compromised owing to the drug resistance and disease recurrence developed in patients with advanced GI (Rottenberg et al., 2021; Behranvand et al., 2022). Therefore, it is vital to discover more effective chemotherapeutics to enhance the efficiency of Pt while reducing side effects.

Effective drug delivery systems (DDSs) based on nano-sized technologies have been proposed recently as a useful strategy for overcoming these issues (Heng, 2018; Unsoy

& Gunduz, 2018; Jain, 2020; Li et al., 2021). Because of their high drug loading capacity, these nanoparticles can efficiently penetrate cancer sites due to their high permeability and retention (Adepu & Ramakrishna, 2021; Zhang et al., 2022). However, despite the enhanced absorption by smart nano-DDSs, P-glycoprotein (P-gp) can still pump intracellular chemotherapy drugs out of cells, causing a reduction in drug concentration inside of cells and compromising chemotherapy efficacy, inducing multidrug resistance (MDR) (Mollazadeh et al., 2018; Waghay & Zhang, 2018). Therefore, blocking the efflux pump function of P-gp directly would be an effective strategy for treating MDR. Recent research has shown that chemotherapy combined with chemodynamic therapy (CDT) is an effective way against MDR (Mollazadeh et al., 2018; Waghay & Zhang, 2018), since CDT can impair the function of P-gp. Thus, MDR cancer cells showed a resurgence of drug sensitivity, namely, the enhanced absorption of cancer drugs caused more apoptosis to occur nearby the cancer cells. Cu<sub>2</sub>O nanoparticles have excellent CDT properties and are reliable drug delivery agents (Chang et al., 2020). In a

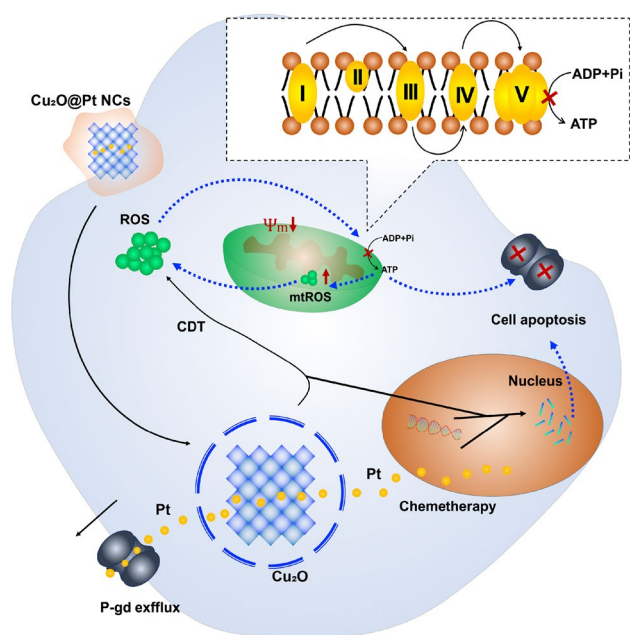
**CONTACT** Tian Lin  [lintian108@163.com](mailto:lintian108@163.com) and Miaosheng Ye  [943706876@qq.com](mailto:943706876@qq.com)

 Supplemental data for this article can be accessed online at <https://doi.org/10.1080/10717544.2022.2121450>

<sup>†</sup>These authors contributed equally to this work.

© 2022 The Author(s). Published by Informa UK Limited, trading as Taylor & Francis Group.

This is an Open Access article distributed under the terms of the Creative Commons Attribution License (<http://creativecommons.org/licenses/by/4.0/>), which permits unrestricted use, distribution, and reproduction in any medium, provided the original work is properly cited.



**Scheme 1.** Schematic illustration of Cu<sub>2</sub>O@Pt-PEG nanosheets for overcome tumor drug resistance.

consistent CDT setting, nano-DDS derived from Cu<sub>2</sub>O could suppress the efflux pump function of P-gp, providing a more effective therapy. The nano-DDS derived from Cu<sub>2</sub>O could directly suppress P-gp's efflux pump function to achieve a better therapeutic effect, when applied with consistent CDT.

In the present study, we developed CDT and chemotherapy by novel nanocrystals (Cu<sub>2</sub>O@Pt NCs). The released Cu ions from the Cu<sub>2</sub>O@Pt NCs could act as Fenton catalyst to boost the generation of reactive oxygen species (ROS) and what's more, under the synergistic effect of Pt, the generation of ROS would increase further. Because of the oxidative stress induced by CDT, the Cu<sub>2</sub>O@Pt NCs were capable of elevating ROS levels and eliciting mitochondrial dysfunction. What's more, P-gp's function could be inhibited by CDT, which reduce cisplatin excretion and reverse drug resistance. *In vivo* results in tumor-bearing mice demonstrated that treatment with Cu<sub>2</sub>O@Pt NCs with CDT and chemotherapy could achieve the most effective antitumor therapeutic effect with the least amounts of adverse effects.

## 2. Experimental section

### 2.1. Materials

Copper chloride dihydrate (CuCl<sub>2</sub>·2H<sub>2</sub>O), polyvinylpyrrolidone (PVP K30, MW = 40 000 Da), sodium hydroxide (NaOH), and ascorbic acid (AA) were purchased from Sinopharm Chemical Reagent Co., Ltd. (Shanghai, China). Cisplatin was obtained from Solarbio (Shanghai, China). Mercapto-polyethylene glycol (SH-PEG, MW = 5000) was acquired from Shanghai Advanced Vehicle Technology (Shanghai, China). Deionized water (DI water, 18.2 MΩ cm) obtained from a Milli-Q water system was used for all experiments. All of the chemicals and reagents were of analytical quality and were utilized without further purification.

### 2.2. Synthesis of Cu<sub>2</sub>O@Pt-PEG nanocrystals

Briefly, the Cu<sub>2</sub>O NCs were made by mixing AA with aqueous Cu<sup>2+</sup> and NaOH and capping them with PVP. Under magnetic stirring, PVP (600 mg) and CuCl<sub>2</sub>·2H<sub>2</sub>O (0.5 mmol) were dissolved in DI water (20 mL), followed by the NaOH aqueous solution (8.0 mmol). In addition, AA (1.0 mmol) was added and then stirred for 20 min. Orange Cu<sub>2</sub>O NCs developed almost immediately with the addition of AA. Centrifugation was used to collect the Cu<sub>2</sub>O NPs, which were then extensively cleaned with DI water and ethanol multiple times.

Second, for modification of PEG, the Cu<sub>2</sub>O NCs (1 mg) and SH-PEG (10 mg) were disseminated in 20 mL DI water under stirring at 60°C for 24 h. The Cu<sub>2</sub>O-PEG NPs were then purified by centrifugation (at 12,000 rpm for 8 min) and kept at 4°C until needed.

Finally, for the synthesis of Cu<sub>2</sub>O@Pt-PEG, Cu<sub>2</sub>O-PEG NCs (1 mg) and cisplatin (1 mg) were combined and agitated for 24 h in ethanol (5 mL). The ethanol was used to wash the precipitate three times. Cu<sub>2</sub>O@Pt-PEG was the name given to the final composite.

### 2.3. Characterization of Cu<sub>2</sub>O@Pt-PEG nanocrystals

A UV-5500PC UV-vis spectrophotometer (Shanghai METASH, China) was used to record UV-vis absorbance spectra. Transmission electron microscope (TEM) images were captured using a JEM-1400F TEM (JOEL) operating at 200 kV. Inductively coupled plasma atomic emission spectrometry (ICP-AES) and atomic absorption spectroscopy (AAS) were used to determine the metal content of the samples using a Prodigy instrument and a HITACHI Z-2300 instrument, respectively. Zeta PALS system (Nanobrook Zeta PALS, Brookhaven Instruments Corporation, USA) was employed to measure the hydrodynamic diameter and zeta.

### 2.4. Intracellular uptake assay

At 37°C and 5% CO<sub>2</sub>, mouse gastric cancer cell (MFC) cells were cultured with 10% fetal bovine serum (FBS) and the rhodamine (Rho)-labeled Cu<sub>2</sub>O@Pt-PEG NCs was added. After incubation, confocal laser scanning microscope (CLSM) was used to observe the cells from 1 to 24 h, and endocytosis of Cu<sub>2</sub>O@Pt-PEG NCs was also observed by CLSM.

### 2.5. In vitro anti-tumor assay

MFC were cultured with 10% fetal bovine serum (FBS) and then treated with Cu<sub>2</sub>O-PEG NCs or Cu<sub>2</sub>O@Pt-PEG NCs for 48 h. The cells were then analyzed using the Live&death assays (Sigma-Aldrich, USA), cell counting kit-8 (CCK-8), and lactate dehydrogenase (LDH) in accordance with the manufacturer's guidelines.

### 2.6. Transwell assays

Transwell plates (BD Biosciences) were used for transwell experiments. A total of 5 × 10<sup>4</sup> cells and 1% FBS were added to each of the upper compartments according to the

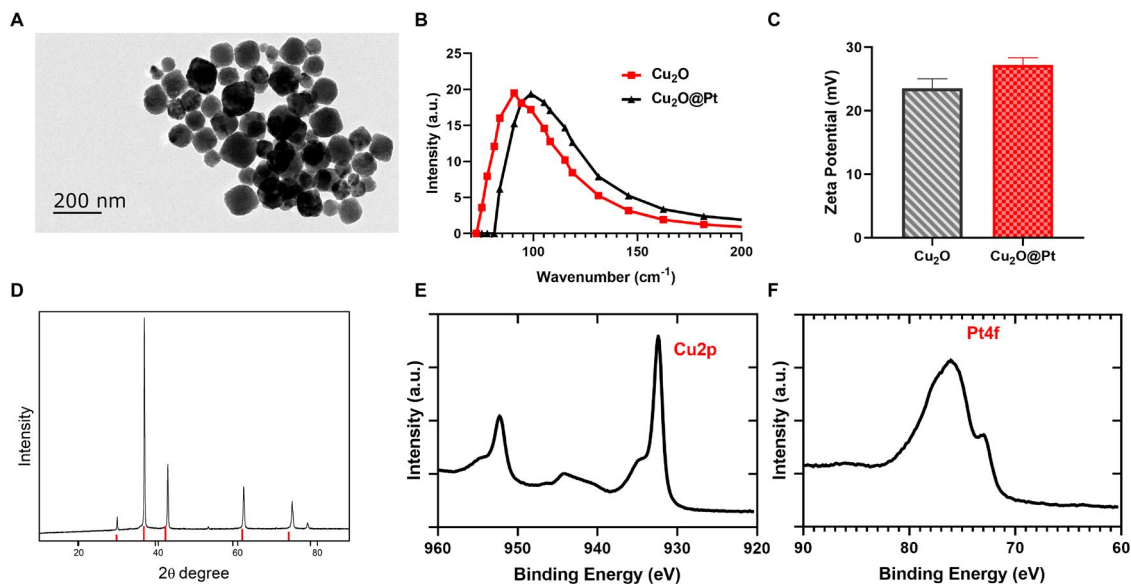


**Figure 1.** A: TEM images  $\text{Cu}_2\text{O}$  NCs; (B) DLS of  $\text{Cu}_2\text{O}$  NCs and  $\text{Cu}_2\text{O@Pt}$  NCs. C: Zeta potential of  $\text{Cu}_2\text{O}$  NCs and  $\text{Cu}_2\text{O@Pt}$  NCs. D: XRD analysis of  $\text{Cu}_2\text{O@Pt}$  NCs; (E) X-ray photoelectron spectroscopy of  $\text{Cu}_2\text{O@Pt}$  NCs, the element of Cu and Pt.

manufacturer's instructions. The lower compartments were induced with 20% FBS. Afterward,  $\text{Cu}_2\text{O}$ -PEG NCs was added to the lower chambers. Taking out the upper compartment after 24 h of incubation at 37°C and fixing the cells in methanol for 30 min was the next step, then the upper surface cells of the upper compartment were removed with cotton swabs. Cells invading to the lower side of the upper compartment were stained with 1% crystal violet.

## 2.7. Measurement of mitochondria damage

Cultured in DMEM with 10% FBS, MFC were seeded and grown for 24 h. Then, the cells were treated with culture medium (set as the blank group) or  $\text{Cu}_2\text{O}$ -PEG NCs for 24 h. To explore anti-tumor mechanism, aforementioned treated cells were also analyzed with ROS (Sigma-Aldrich), Rho123 assay, mitochondrial ROS (mitoROS; AAT Bioquest, Wuhan, China), mitochondrial permeability transition pore (MPTP) kit (BestBio, Shanghai, China), JC-1 kit (Keygen, Nanjing, China), and mitochondrial complex I-V (Solarbio, Beijing, China).

## 2.8. In vivo anti-tumor study

To construct a tumor-bearing BALB/c mouse model, harvested MFC were suspended in a suitable amount of PBS. The mice were then injected with 50 mL of suspension in their left flank. When the tumor volume reached 50 mm<sup>3</sup>, six groups of mice were divided, which were treated with saline (negative control), Cisplatin (2 mg/kg, Low dose), Cisplatin (5 mg/kg, high dose), and  $\text{Cu}_2\text{O}$ -PEG NCs or  $\text{Cu}_2\text{O@Pt}$ -PEG NCs solutions via tail vein injection every 2 days. The tumor volumes were recorded daily for 14 days.

### 2.8.1. In vivo biosafety and metabolism study

$\text{Cu}_2\text{O@Pt}$ -PEG NCs were intravenously injected separately into the healthy BALB/c mice for investigating the in vivo Biosafety

and Metabolism of  $\text{Cu}_2\text{O@Pt}$ -PEG NCs. A digestion solution containing digesting aqua regia was used at the indicated time points (0 h, 6 h, 12 h, 24 h) for collecting, weighing, and dissolving the main organs and tumor. The concentrations of Cu ions in different samples were detected by ICP-MS. Meanwhile, main organs (heart, liver, spleen, lung, and kidney) were obtained for H&E staining.

## 2.9. Statistical analysis

Results are expressed as mean  $\pm$  standard deviation (SD). Except where indicated otherwise, all tests have been repeated three times and produced comparable results. Unpaired *t* tests were used to examine statistical data, analysis of variance, and Student's *t* tests (ANOVA). At  $p < .05$ , differences were judged statistically significant.

## 3. Results and discussion

### 3.1. Synthesis of $\text{Cu}_2\text{O@Pt}$ -PEG nanocrystals

Figure 1(A) shows a cubic morphology with an average diameter of 75 nm for  $\text{Cu}_2\text{O}$  by the TEM. As shown in Figure 1(B), dynamic light scattering (DLS) measurement found that the hydrodynamic size (Dh) of the  $\text{Cu}_2\text{O}$  and  $\text{Cu}_2\text{O@Pt}$  NCs were respectively  $84.41 \pm 2.01$  nm and  $102.32 \pm 2.34$  nm. Results from zeta potential showed  $24.31 \pm 2.00$  mV and  $29.46 \pm 1.52$  mV for  $\text{Cu}_2\text{O}$  NCs and  $\text{Cu}_2\text{O@Pt}$  NCs, indicating the feasibility for biomedical applications (Figure 1(C)). What's more, powder X-ray diffraction (XRD) analysis was used to establish the chemical composition and phase structure of  $\text{Cu}_2\text{O}$ ; every reflection peaks were compatible with cubic  $\text{Cu}_2\text{O}$  (Chang et al., 2020) (Figure 1(D)). Meanwhile, X-ray photoelectron spectroscopy (XPS) confirmed that Cu and Pt were the main elements inside  $\text{Cu}_2\text{O@Pt}$ , suggesting the NCs were pure (Figure 1(E,F)). The content of Pt and Cu, determined by

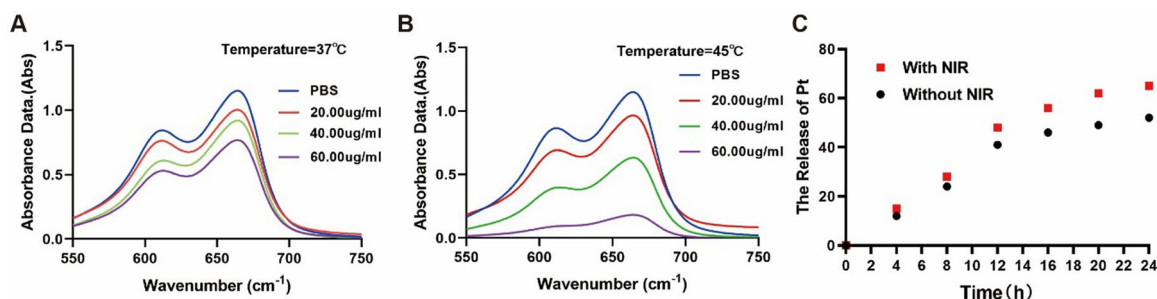


**Figure 2.** Fenton-like properties assessed by MB in the presence of Cu<sub>2</sub>O NPs at different concentrations at (A) 37°C and (B) 50°C; (C) time-dependent Pt release from the Cu<sub>2</sub>O@Pt NPs with and without NIR.

inductively coupled plasma mass spectrometry, was 3.5% and 24.5%, respectively.

### 3.2. Characterization of Cu<sub>2</sub>O@Pt-PEG nanocrystals

To determine whether Cu<sub>2</sub>O@Pt-PEG produce Fenton-like effect, MB assays based on MB degradation were used (Wu et al., 2020). In the presence of high concentrations of Cu<sub>2</sub>O@Pt-PEG, MB absorption decreased, indicating abundant ·OH production by Cu<sub>2</sub>O@Pt-PEG NPs (Figure 2(A)). In accordance with previous reports, the results were positive (Chang et al., 2020; Gao et al., 2022). Moreover, to investigate the role of temperature in the Fenton-like reactions of the Cu<sub>2</sub>O@Pt-PEG NPs, we placed the reaction systems in a water bath at 50°C. In a water bath at 50°C, the Cu<sub>2</sub>O@Pt-PEG NPs had a lower MB absorption than those at 37°C (Figure 2(B)). The Cu<sub>2</sub>O@Pt-PEG NPs solution (120 mg/mL) demonstrated a 10-fold enhancement at 50°C when compared to those at 25°C. The results showed that increased temperature could significantly improve the Fenton-like effect of Cu<sub>2</sub>O@Pt-PEG NPs, suggesting a more effective method of CDT by mild photothermal treatment. To detect the ability to release Pt, the boosted Pt from Cu<sub>2</sub>O@Pt-PEG nanoparticles was assessed by ICP-AES. As shown in Figure 2(C), more than 50% of the Pt was produced within 24 h. Meanwhile, Cu<sub>2</sub>O@Pt-PEG NPs released more Pt with NIR, resulting in more effective chemotherapy effects. What's more, to simulate acidic tumor microenvironment, we conducted the supplement experiment to explore the release studies of Pt and Cu in the PBS and in a solution with low pH. As shown in the Supplementary Figure S1, Cu<sub>2</sub>O@Pt-PEG NPs released more Pt with low pH (Supplementary Figure S1(A)) and the experiment for Cu had similar results (Supplementary Figure S1(B)). As a result, Pt could better diffuse from the Cu<sub>2</sub>O@Pt NPs due to thermodynamic effects, which are consistent with the previous study.

### 3.3. In Vitro cellular uptake and anti-tumor effect of Cu<sub>2</sub>O@Pt-PEG nanocrystals

Platinum (Pt) including cisplatin, oxaliplatin, and carboplatin, which refers to Pt(II) drug, have been preferred as first-line agents for the chemotherapy of patients with GI tumor (Johnstone et al., 2013; Chau et al., 2016; Dilruba & Kalayda, 2016; Yang et al., 2020). Chemotherapy mainly induces

caspase-dependent apoptosis within cancer cells, while long-term exposure leads to enhanced anti-apoptosis signal or decreased drug sensitivity (Carneiro & El-Deiry, 2020). However, it is very difficult for intravenously injected chemo-agents to selectively enter tumor region during the blood circulation process (Bregni et al., 2020). To achieve better therapeutic effects, clinicians often choose to using high dose of drugs for treatment, while this regimen is prone to cause systemic side effects, which may lead to the failure to tolerate and discontinue treatment for patients with cancer.

Therefore, it is a very important issue for efficient drug delivery during GI cancer therapy. Inspired by the fact that nanosized DDSs have evolved to fully adapt to tumor surroundings owing to enhanced permeability and retention (EPR) effect (Kobayashi et al., 2013; Goos et al., 2020), Cu<sub>2</sub>O-PEG nanocarriers were applied for the delivery of Pt. To verify that, the cellular uptake Cu<sub>2</sub>O@Pt-PEG NPs were performed using CLSM, which were pre-labeled with rhodamine (Rho). From CLSM images, it could be observed that the cellular uptake of Cu<sub>2</sub>O@Pt-PEG NPs was at a time-dependent manner. Especially, visible red fluorescence in cancer cells could be significantly observed only after 4 h of incubation. Cancer cells showed the stronger red fluorescence after 8 h of incubation and only when the incubation time reached 12 h, did the accumulated Rho fluorescence in the cytoplasm eventually reach a very high level, which could be obviously understood by corresponding quantitative analysis. In particular, we could find no significant increase of Rho fluorescence at the incubation time of 24 h, compared to 12 h, indicating that 12 h was the highest cellular uptake time (Figure 3(A), Supplementary Figure S2). Given the excellent cellular uptake and Fenton-like catalytic activities of Cu<sub>2</sub>O@Pt-PEG, we then performed CCK-8 and LDH assay to evaluate their anti-tumor effect. From CCK-8 results, cell viability rate of cancer cells declined for all groups at dose-dependent manner, but at a totally different slope. When the concentration of Pt was 16 µg/mL, Pt (~30%) and Cu<sub>2</sub>O-PEG (~30%) showed more significant inhibitory effect to cancer cells. Interestingly, Cu<sub>2</sub>O@Pt-PEG (refer to chemo/CDT) caused twofold changes higher cell toxicity (~80%) than Pt and Cu<sub>2</sub>O-PEG (Figure 3(B)). Consistently, LDH as a cell damage assay showed that with increasing concentration, LDH decreased in Pt, Cu<sub>2</sub>O-PEG, and Cu<sub>2</sub>O@Pt-PEG treated groups, whereas the LDH rate was more evident in the Cu<sub>2</sub>O@Pt-PEG group (Figure 3(C)). Therefore, CCK-8 and LDH assay

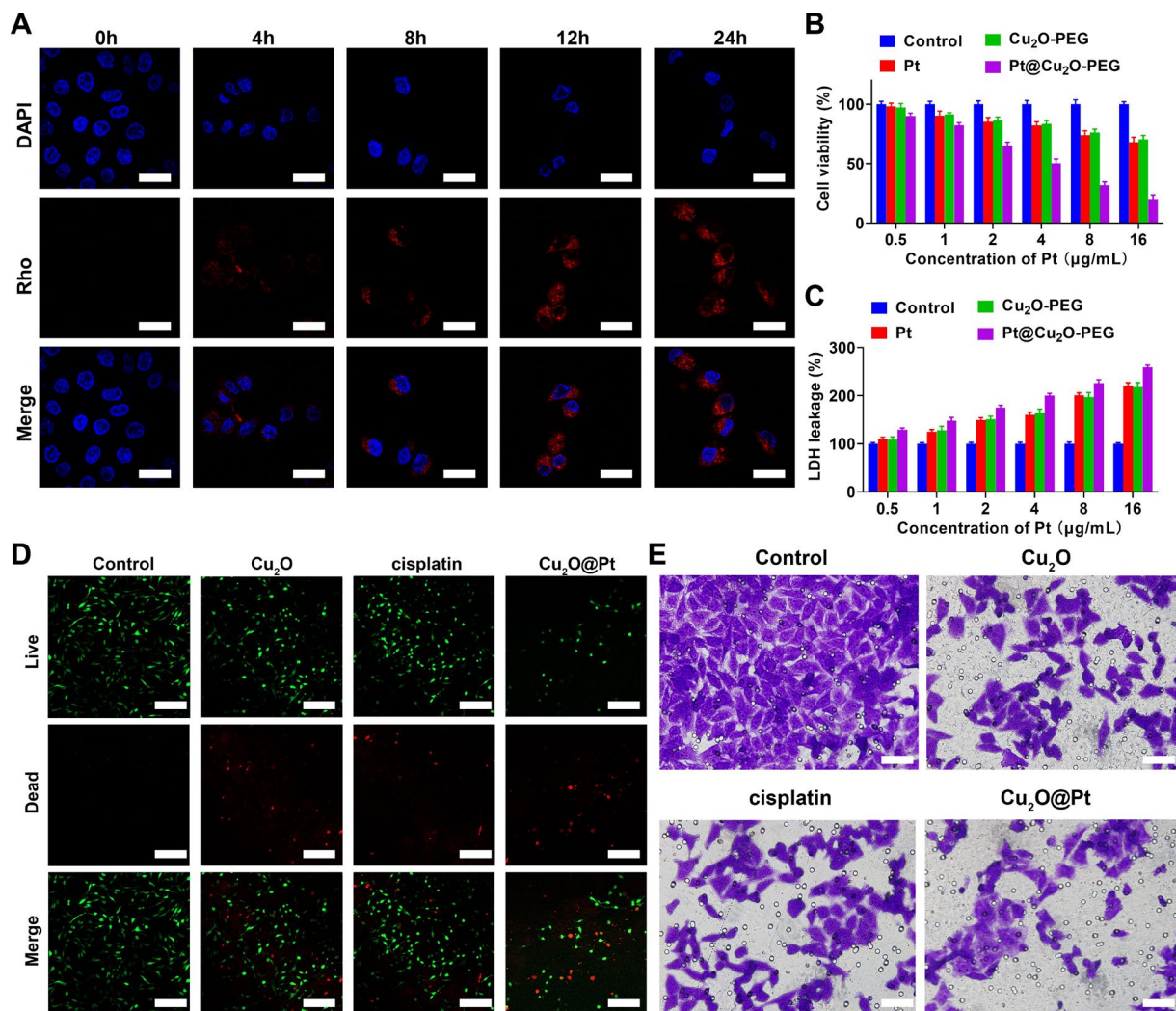


**Figure 3.** A: CLSM images of MFC cells treated with Cu<sub>2</sub>O@Pt-PEG NCs for 1–8 h. Scale bar: 20 µm. B: CCK-8 assay of MFC cells after treated with Cu<sub>2</sub>O-PEG and Cu<sub>2</sub>O@Pt-PEG. C: LDH leakage assay of MFC cells after treated Cu<sub>2</sub>O-PEG and Cu<sub>2</sub>O@Pt-PEG. D: Live&Dead images of MFC cells after treatment. Scale bar: 100 µm. E: Transwell assay of MFC cells after treated Cu<sub>2</sub>O-PEG and Cu<sub>2</sub>O@Pt-PEG.

indicated that synthetic chemo/CDT effects of Cu<sub>2</sub>O@Pt-PEG NCs showed a much better results than those single chemotherapy (Pt) or single CDT effect (Cu<sub>2</sub>O-PEG).

To detect the chemo/CDT-therapeutic effectiveness, incubation of cancer cells with Cu<sub>2</sub>O@Pt-PEG (8 µg/mL of Pt) was managed for further experiments. Compared with cell-impermeable Propidium Iodide (PI) that could merely stain the dead cells' nuclei with strong red fluorescence, low toxic calcein-AM could penetrate a living cell membrane, while being hydrolyzed into calcein and brightening green fluorescence (Uggeri et al., 2004). As shown in live&death results, Pt, Cu<sub>2</sub>O-PEG, and Cu<sub>2</sub>O@Pt-PEG treatments all demonstrated reduced green intensity, accompanied with increased red intensity (Figure 3(D), Supplementary Figure S3). Furthermore, Transwell assay results revealed that significantly Pt, Cu<sub>2</sub>O-PEG, and Cu<sub>2</sub>O@Pt-PEG attenuated the migratory ability of cancer cells compared with control group (Figure 3(E), Supplementary Figure S4). To date, Cu<sub>2</sub>O@Pt-PEG did showed most decreased green intensity and upregulated red intensity in live&death research, and most suppressed migrated cell numbers in Transwell experiments. The

forementioned results suggested Cu<sub>2</sub>O@Pt-PEG NPs not only possesses great toxicity, but also to bust anti-proliferation and anti-metastasis effect to cancer cells.

### 3.4. CDT effect induced by Cu<sub>2</sub>O@Pt-PEG could reverse drug resistance by decreasing mitochondria-derived ATP

Though the excellent anti-tumor effect of Cu<sub>2</sub>O@Pt-PEG NCs has been proved, the mechanism is still unclear. In spite of smart DDSs enhancing absorption, P-glycoprotein (P-gp) has been shown to pump out chemoagents endocytosed by cancer cells (Mollazadeh et al., 2018). ATP-binding cassette (ABC) transporters such as P-gp, which have a molecular mass of 170 kD, act as 'drug pumps' that consume ATP (Leopoldo et al., 2018). In general, the efflux of intracellular drugs via energy-dependent P-gp causes the concentration of drugs inside the cell to decrease and the development of resistance to those drugs (Waghray & Zhang, 2018). Accordingly, reducing ATP supplements could be a promising strategy for suppressing P-gp's efflux pump function and the

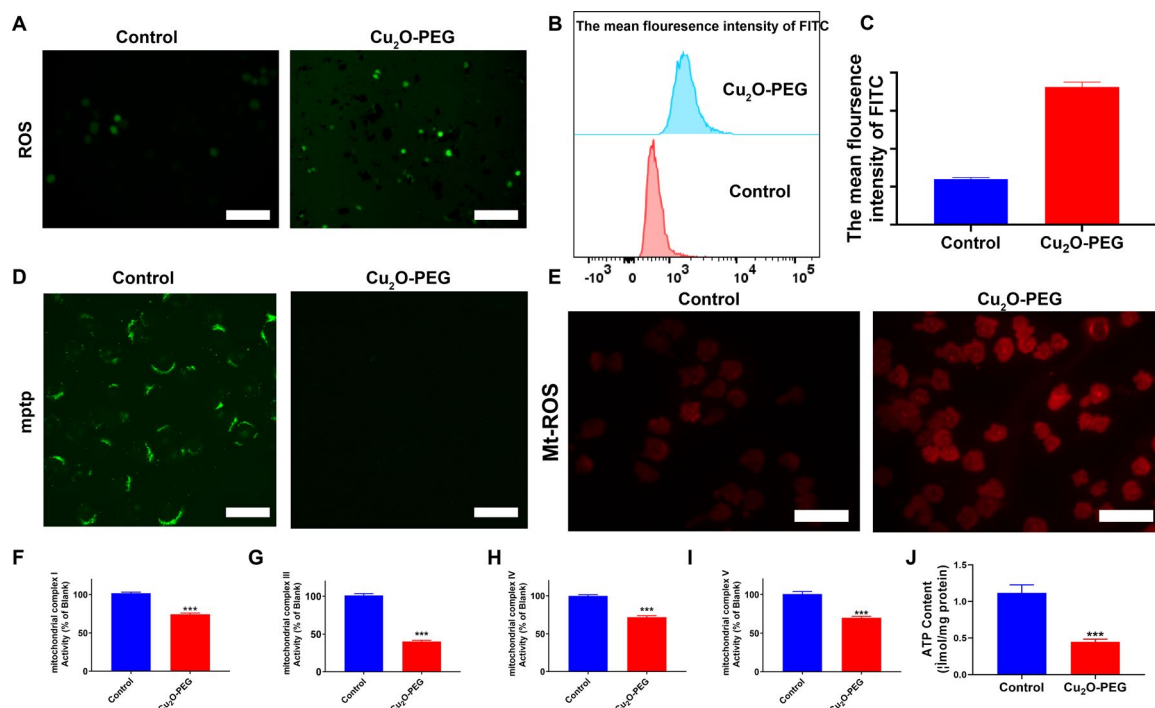


**Figure 4.** A: Total ROS image of MFC cells after treated with PBS (Control) and  $\text{Cu}_2\text{O}$ -PEG. Scale bar: 100  $\mu\text{m}$ . B and C: Quantified plot of Rho content in MFC cells, detected by flow cytometry; (D) MPTP images of MFC cells after treatment with PBS (Control) and  $\text{Cu}_2\text{O}$ -PEG. Scale bar: 20  $\mu\text{m}$ . E: Total Mt-ROS image of MFC cells after treated with PBS (Control) and  $\text{Cu}_2\text{O}$ -PEG. Scale bar: 50  $\mu\text{m}$ . F–I: The activities of complexes I/III/IV/V of MFC cells after treated with  $\text{Cu}_2\text{O}$ -PEG. J: ATP production of MFC cells after treated with  $\text{Cu}_2\text{O}$ -PEG.

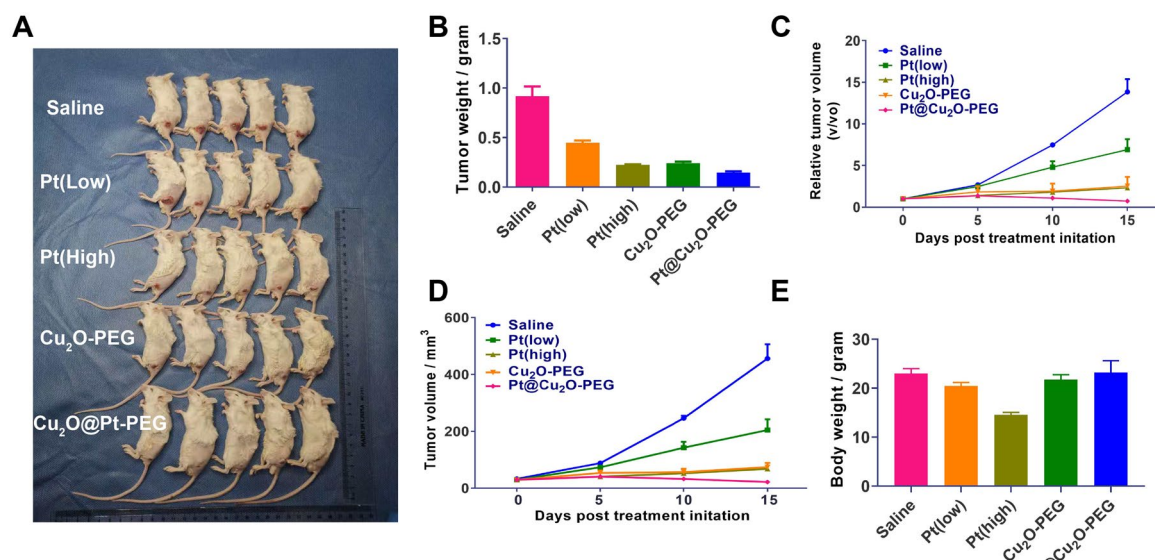


**Figure 5.** *In vivo* therapeutic properties of  $\text{Cu}_2\text{O}$ @Pt-PEG NPs. A: Images of the primary tumors derived from mice with different treatments. B: Body weights following the recommended procedures. C: Tumor volumes and Relative tumor volumes (D) after the recommended remedies. E: Tumor weights after the indicated treatments.

reversal of drug delivery. In addition, the complex enzymatic activities of the mitochondrial respiratory chain determine intracellular ATP production. It has been demonstrated that the inevitable product of cellular metabolism, ROS, can cause mitochondrial damage (Yang et al., 2019), whereas the CDT effect can increase ROS levels inside the cells (Tang et al., 2019). According to that, we assumed that these  $\text{Cu}_2\text{O}$ @Pt-PEG NPs might stimulate the intracellular generation of ROS and trigger mitochondrial damage via its CDT effect.

Consequently, both ATP synthesis and the efflux pump ability of P-gp might be dysfunctional due to the insufficient energy supplement.

To confirm this, we treated cancer cells with our designed  $\text{Cu}_2\text{O}$ -PEG NCs first and detected their ROS generation ability. After the intervention, ROS generation in  $\text{Cu}_2\text{O}$ -PEG-treated cells was remarkably increased, which was exhibited via DCFH-DA, a biological probe to detect the intracellular levels of ROS (Figure 4(A), Supplementary Figure S5). To further

explore the ability of retention of intracellular drugs, the cancer cells were treated with our designed Cu<sub>2</sub>O-PEG NCs first and detected the ability of Rho123 retention, which showed the ability of drug retention in the cells. After the intervention, the fluorescence of Rho123 in Cu<sub>2</sub>O@Pt-PEG-treated cells was remarkably increased, indicating the dysfunctional efflux pump of P-gp (Figure 4(B), Supplementary Figure S6). Apart from this, the matrix metalloproteinase (MMP) were detected by JC-1 kit and the group with Cu<sub>2</sub>O-PEG NCs collapsed sharply (Figure 4(C), Supplementary Figure S7). The results also revealed that Cu<sub>2</sub>O-PEG NCs further enhanced the opening of mPTP, with a sharp decrease in microsomal triglyceride transfer protein (MTP) (Figure 4(D), Supplementary Figure S8). Therefore, our results elucidate that the CDT effect induced by Cu<sub>2</sub>O-PEG NPs could destroy mitochondria. Subsequently, MitoSOX Red was applied to discern superoxide as an indicator in mitochondria using CLSM analysis, to illuminate whether the generated ROS could cause inner mitochondrial damage. Notably, red fluorescence (mitochondrial ROS, also called mitoROS) was rapidly increased in the Cu<sub>2</sub>O-PEG-treated group (Figure 4(E), Supplementary Figure S9). Moreover, we found that Cu<sub>2</sub>O-PEG NPs also reduced the activities of complexes I/III/IV/V in treated cancer cells, indicating Cu<sub>2</sub>O-PEG NPs generated ROS injured NADH-dependent Electron transport chain (ETC). The procedure of ATP generation was evidently suppressed because of the damage to mitochondria complexes (Figure 4(F-I)). Subsequently, more Rho123 was sequestered, indicating the dysfunctional efflux pump of P-gp. These results indicated mitochondrial-complexes I/III/IV/V chain in Cu<sub>2</sub>O-PEG NPs-treated cells was damaged, resulting in ATP production decline and dysfunction of P-gp pumps (Figure 4(J)).

### 3.5. Biosafety and metabolism study and anti-Tumor efficiency of Cu<sub>2</sub>O@Pt-PEG nanocrystals *in vivo*

To explore the biosafety and *in vivo* metabolism of inorganic nanomaterials, relevant experiment have been conducted. As demonstrated in Supplementary Figure S10, the Cu<sub>2</sub>O@Pt-PEG NPs are injected intravenously, it was primarily taken up by liver, spleen, kidney, and tumor, and they are gradually processed and eliminated by liver and kidney after 24h. In addition, tissues stained with H&E were used to evaluate the biosafety of Cu<sub>2</sub>O@Pt-PEG NPs in the treatment of major organs, and no inflammation or damage was observed (Supplementary Figure S11).

We have confirmed that Cu<sub>2</sub>O@Pt-PEG can effectively exert anti-tumor effects *in vitro*, and then we further tested the anti-tumor effect of Cu<sub>2</sub>O@Pt-PEG on tumor-bearing mice, which were treated with Pt (low dose), Pt (high dose), Cu<sub>2</sub>O-PEG or Cu<sub>2</sub>O@Pt-PEG (with a low dose of Pt), and saline (negative control) every 2 days. The results of *in vivo* experiments showed that the tumor volumes and tumor weights in Pt (low dose), Pt (high dose), Cu<sub>2</sub>O-PEG and Cu<sub>2</sub>O@Pt-PEG (with low dose of Pt) groups did being significantly reduced, compared to those in saline group. Among all, Pt (low) showed a ~50% inhibitory effect, which was much less than those in Pt (high) group with a ~65% inhibitory response. To date, Cu<sub>2</sub>O-PEG also showed well anti-proliferation capacity (~70%),

whereas the combination effect of chem plus CDT resulted from Cu<sub>2</sub>O@Pt-PEG, showed most efficient anti-growth effect to tumor (Figure 5(A,C-E)). Apart from this, the safety of anti-cancer drugs is an important consideration in clinical research. To further evaluate their potential side effects, we tested the weight change of mice throughout the experiment, and the results showed that the weight changes of Cu<sub>2</sub>O-PEG and Cu<sub>2</sub>O@Pt-PEG groups of mice were not statistically different from control group. However, both Pt-treated groups showed significant decreased body weight, whereas Pt (high) demonstrated lower body weights compared to Pt (low). This phenomenon indicates that Pt chemo-agents showed dose-dependent side toxicity to mice, while Cu<sub>2</sub>O-PEG and Cu<sub>2</sub>O@Pt-PEG has no significant side effects (Figure 5(B)).

All results aforementioned implied that Cu<sub>2</sub>O@Pt-PEG had a remarkable antitumor effect and the laser could enhance this antitumor effect *in vivo*. In summary, Cu<sub>2</sub>O@Pt-PEG has good prospects in the treatment of cancer.

## 4. Conclusions

In conclusion, we developed novel nanocrystals (Cu<sub>2</sub>O@Pt NCs) to overcome drug resistance by reducing mitochondria-derived ATP through chemo/CDT in GI cancer. The Cu<sub>2</sub>O@Pt NCs were able to carry out CDT. Because of the oxidative stress induced by CDT, the Cu<sub>2</sub>O@Pt NCs were capable of elevating ROS levels and eliciting mitochondrial dysfunction and furthermore, the release of cisplatin further impaired mitochondrial function. What's more, P-gp's function could be inhibited by the reduction of mitochondria-derived ATP through chemo/CDT, which reduce cisplatin excretion and reverse drug resistance. *In vivo* results in tumor-bearing mice demonstrated that treatment with Cu<sub>2</sub>O@Pt NCs with CDT and chemotherapy could achieve the most effective antitumor therapeutic effect with the least amounts of adverse effects (Scheme 1).

## Data availability statement

The datasets used in the present study are available from the corresponding author upon reasonable request.

## Disclosure statement

The authors declare no competing financial interest.

## Funding

The work is supported by the Medical and Health Science and Technology Project of Zhejiang Province (2020RC121) and 2019 Jiaying Key Discipline of Medicine Oncology Supporting Subject (2019-zc-11).

## References

- Adepu S, Ramakrishna S. (2021). Controlled drug delivery systems: current status and future directions. *Molecules* 26:5905.
- Akahoshi K, Oya M, Koga T, Shiratsuchi Y. (2018). Current clinical management of gastrointestinal stromal tumor. *World J Gastroenterol* 24:2806–17.

- Behranvand N, Nasri F, Zolfaghari ER, et al. (2022). Chemotherapy: a double-edged sword in cancer treatment. *Cancer Immunol Immunother* 71:507–26.
- Bray F, Ferlay J, Soerjomataram I, et al. (2018). Global cancer statistics 2018: GLOBOCAN estimates of incidence and mortality worldwide for 36 cancers in 185 countries. *CA Cancer J Clin* 68:394–424.
- Bregni G, Akin TT, Camera S, et al. (2020). Adjuvant chemotherapy for rectal cancer: Current evidence and recommendations for clinical practice. *Cancer Treat Rev* 83:101948.
- Carneiro BA, El-Deiry WS. (2020). Targeting apoptosis in cancer therapy. *Nat Rev Clin Oncol* 17:395–417.
- Chang M, Hou Z, Jin D, et al. (2020). Colorectal tumor microenvironment-activated bio-decomposable and metabolizable  $\text{Cu}_2\text{O}@\text{CaCO}_3$  nanocomposites for synergistic oncotherapy. *Adv Mater* 32:e2004647.
- Chau LY, Qijin H, Ailin Q, et al. (2016). Platinum nanoparticles on reduced graphene oxide as peroxidase mimetics for the colorimetric detection of specific DNA sequence. *J Mater Chem B* 4:4076–83.
- Chen X, Wang H, Huang Y, et al. (2021). Future perspectives of exosomes in peritoneal metastasis of gastric cancer. *Front Oncol* 2021;11.
- Dilruba S, Kalayda GV. (2016). Platinum-based drugs: past, present and future. *Cancer Chemother Pharmacol* 77:1103–24.
- Gao L, Song Y, Zhong J, et al. (2022). Biocompatible 2D Cu-TCPP nanosheets derived from  $\text{Cu}_2\text{O}$  nanocubes as multifunctional nanoplatforms for combined anticancer therapy. *ACS Biomater Sci Eng* 8:1074–86.
- Goos JACM, Cho A, Carter LM, et al. (2020). Delivery of polymeric nano-stars for molecular imaging and endoradiotherapy through the enhanced permeability and retention (EPR) effect. *Theranostics* 10:567–84.
- Heng P. (2018). Controlled release drug delivery systems. *Pharm Dev Technol* 23:833.
- Jain KK. (2020). An overview of drug delivery systems. *Methods Mol Biol* 2059:1–54.
- Johnstone TC, Wilson JJ, Lippard SJ. (2013). Monofunctional and higher-valent platinum anticancer agents. *Inorg Chem* 52:12234–49.
- Kobayashi H, Watanabe R, Choyke PL. (2013). Improving conventional enhanced permeability and retention (EPR) effects; what is the appropriate target? *Theranostics* 4:81–9.
- Leopoldo M, Nardulli P, Contino M, et al. (2018). An updated patent review on P-glycoprotein inhibitors (2011–2018). *Expert Opin Ther Pat* 29:455–61.
- Li Q, Zhou Y, He W, et al. (2021). Platelet-armed nanoplatform to harmonize janus-faced IFN-gamma against tumor recurrence and metastasis. *J Control Release* 338:33–45.
- Mollazadeh S, Sahebkar A, Hadizadeh F, et al. (2018). Structural and functional aspects of P-glycoprotein and its inhibitors. *Life Sci* 214:118–23.
- Rottenberg S, Disler C, Perego P. (2021). The rediscovery of platinum-based cancer therapy. *Nat Rev Cancer* 21:37–50.
- Sung H, Ferlay J, Siegel RL, et al. (2021). Global Cancer Statistics 2020: GLOBOCAN estimates of incidence and mortality worldwide for 36 cancers in 185 countries. *CA Cancer J Clin* 71:209–49.
- Tang Z, Liu Y, He M, Bu W. (2019). Chemodynamic therapy: tumour microenvironment-mediated fenton and fenton-like reaction. *Angew Chem Int Ed Engl* 58:946–56.
- Uggeri J, Gatti R, Belletti S, et al. (2004). Calcein-AM is a detector of intracellular oxidative activity. *Histochem Cell Biol* 122:499–505.
- Unsoy G, Gunduz U. (2018). Smart drug delivery systems in cancer therapy. *Curr Drug Targets* 19:202–12.
- Venerito M, Link A, Rokkas T, Malfertheiner P. (2016). Gastric cancer – clinical and epidemiological aspects. *Helicobacter* 21:39–44.
- Waghay D, Zhang Q. (2018). Inhibit or evade multidrug resistance P-glycoprotein in cancer treatment. *J Med Chem* 61:5108–21.
- Wu H, Chen F, You C, et al. (2020). Smart porous core-shell cuprous oxide nanocatalyst with high biocompatibility for acid-triggered chemo/chemodynamic synergistic therapy. *Small* 16:e2001805.
- Yang B, Chen Y, Shi J. (2019). Reactive oxygen species (ROS)-based nanomedicine. *Chem Rev* 119:4881–985.
- Yang Y, Yu Y, Chen H, et al. (2020). Illuminating platinum transportation while maximizing therapeutic efficacy by gold nanoclusters via simultaneous near-infrared-I/II imaging and glutathione scavenging. *ACS Nano* 14:13536–47.
- Zhang M, Qin X, Zhao Z, et al. (2022). A self-amplifying nanodrug to manipulate the Janus-faced nature of ferroptosis for tumor therapy. *Nanoscale Horiz* 7:198–210.